

# NOVEL PERMANENT MAGNET LINEAR GENERATOR TOPOLOGY FOR WAVE ENERGY CONVERSION

R. Vermaak\*, M.J. Kamper†

Department of Electrical and Electronic Engineering,  
University of Stellenbosch, Private Bag X1, 7602, Matieland, South Africa.

\*rvermaak@ieee.org, †kamper@sun.ac.za

**Keywords:** Concentrated coil, direct drive, linear generator, permanent magnet, wave energy converter.

## Abstract

A novel topology for a permanent magnet linear generator for wave energy conversion is proposed. It aims to increase power density and to eliminate uneven air gap flux distribution caused by the longitudinal ends; this is done by eliminating stator and rotor yokes and by introducing a new flux path. Analytical and FEM studies are used to analyse the concept and to compare it to existing machines. Results and design challenges are discussed.

## 1 Introduction

A vast amount of energy is contained in the world's oceans in the form of waves. However, the technology for wave energy converters (WECs) is still relatively undeveloped [4] and most WECs are still in the development stage. Some of the most important WECs are discussed in [8]. Among these, direct drive devices employing permanent magnet (PM) linear generators have the advantage of eliminating any kind of mechanical interface between the device and the electrical generator. This reduces the need for maintenance, increases efficiency and contributes to the WEC's robustness, all of which are important features for the hostile environment of the ocean. Due to the slow speed of the waves, the generated power is mostly dependent on the generator force, which in turn is dependent on the machine's active air gap area [10]. This leads to large, expensive machines. Strong attraction forces between iron stators and PM translators also cause problems in bearing design [10] and increased structural mass [8].

Different concepts and topologies for linear generators have recently been summarised comprehensively in [8, 10]. Of these, the conventional longitudinal flux synchronous PM linear generator with an iron stator is the most widely used, e.g. as used in the AWS, Uppsala University device and Oregon State University (OSU) device. These generators have ideal flux paths as shown in Fig. 1. The magnetic flux is produced by the PMs on the translator. The flux crosses the air gap, flows through the stator teeth and yoke, back through the two adjacent, oppositely polarised poles and the translator back yoke. In this ideal situation, and as also happens in rotary machines, the flux from one pole couples equally with each of its

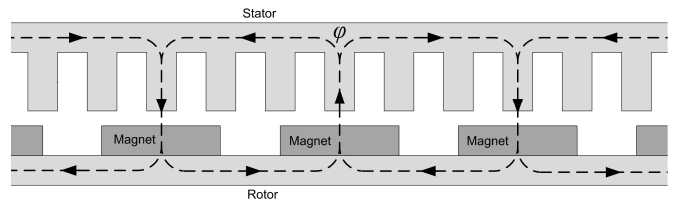


Figure 1: Ideal flux path through a conventional machine.

adjacent poles. However, in practise, the longitudinal ends of linear generators have an interesting effect on the flux paths through the machine. As shown in Fig. 2, the flux of the edge magnet at the longitudinal end couples almost completely with the neighbouring magnet, causing a pair-wise coupled flux pattern [3]. Due to saturation and symmetry, this flux distribution progressively evens out towards the middle of the PM translator, causing an uneven flux distribution in the air gap. This could have an adverse effect on the performance of the machine [3].

New concepts involving double-sided PM translators and air-cored stators have recently been investigated [5, 6] mostly as a way of eliminating the strong attraction forces between the stator and translator. Non-overlapping concentrated coil windings used in these configurations are also shown to significantly reduce copper mass compared to overlapping windings, simplify construction efforts and increase efficiency [6]. A new idea proposed in [5] is also to isolate neighbouring pole pairs from each other and to force the flux through the so-called 'C'-core as shown in Fig. 3. This helps to reduce inactive structural mass.

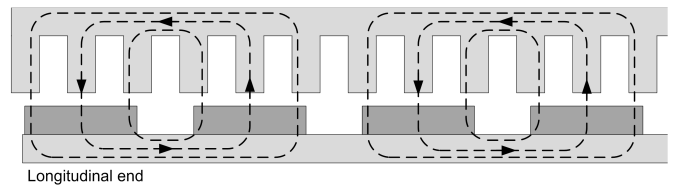


Figure 2: Pair-wise flux coupling due to longitudinal ends.

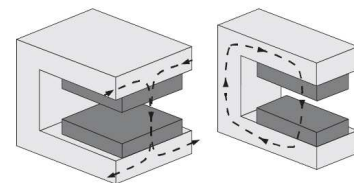


Figure 3: Flux paths through 'C'-core pole modules [5].

In this paper a novel topology for a linear PM generator is proposed. In Section 2 this topology is introduced, after which the design of the machine is considered. Case studies of air-cored machines are done and comparisons made with existing machines.

## 2 Proposed linear generator topology

The proposed generator concept can be seen in Fig. 4. A series of double sided translators are arranged in a tubular topology. The yokes are removed so that each pair of adjacent rows of magnets can be replaced with one row of magnets. Without a steel yoke, eddy-current losses usually present in the yoke are eliminated [9]. The net attraction force on any particular magnet is ideally zero, as each magnet will experience the same force from both sides. The flux now also circulates around the translator in the x-y plane (see Fig. 4 and Fig. 5), and hence no pair-wise flux coupling between adjacent poles is experienced and the air gap flux distribution is even.

The stator consists of many individual sections which are connected in series or in parallel. These can be manufactured separately and easily inserted from the outside. The stator is also yoke-less and hence the armature reaction effect is small. This reduces eddy-current losses in the magnets and also means that the machine has a very low internal reactance, and hence a small load angle.

Non-overlapping concentrated coil windings are used; the advantages of this have already been explained. Both air-cored and iron-cored stators can be implemented. Ideally, due to the double-sided rotor configuration, the net force on an iron-cored stator should also be zero. It is noted in the literature [8, 10], though, that due to manufacturing tolerances, this is not the case and that the double-sided configuration in practice only serves to *reduce* the net force on the stator. With this topology it is also expected to have a greater active air gap area per unit volume than other topologies, which would serve to increase the machine's power density.

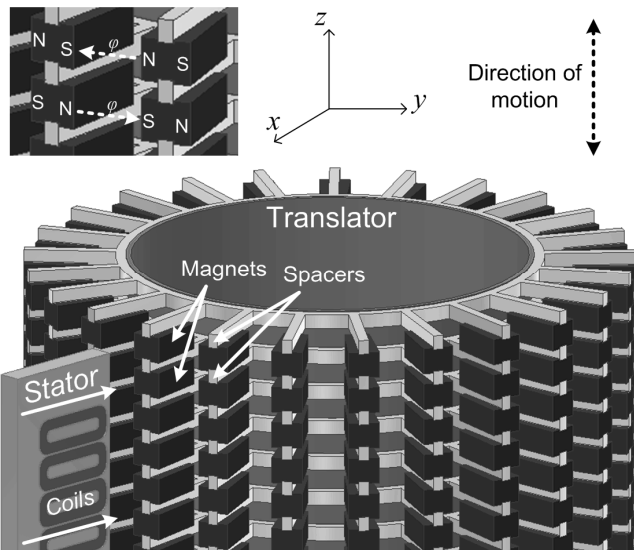


Figure 4: Novel linear machine topology.

## 3 Design considerations

The case studies in Section 4 are done for air-cored machines, and hence only the design aspects of air-cored machines are considered here.

### 3.1 Air gap area and shear stress.

The power  $P_d$  generated by a linear generator WEC can be expressed as

$$P_d = f_s v_s, \quad (1)$$

where  $f_s$  is the generator force and  $v_s$  is the translator velocity. Since the wave speed varies roughly sinusoidally, the instantaneous power produced from a three phase linear generator also varies sinusoidally. For the design, a constant speed equal to the average vertical speed of the waves is assumed. This speed is however a given parameter and cannot be controlled. The shear force  $f_s$ , tangential to the air gap area  $A_g$ , produced by the machine therefore controls the power generated. The shear force in turn depends on the air gap flux density and the current, according to

$$f_s = \sigma_s A_g = \left(\frac{1}{2} B_p K_p\right) A_g, \quad (2)$$

where  $\sigma_s$  is the shear stress in  $N/m^2$ ,  $B_p$  is the peak air gap flux density in tesla and  $K_p$  is the peak electric loading of the machine in A/m. Both  $B_p$  and  $K_p$  are limited to certain values. It is therefore essential to maximise the active air gap area of the machine in order to produce maximum power.

The air gap area for the new topology will depend on the number of stator sections  $n_s$  that can be arranged around the translator. The number of stator sections is determined by the inner radius  $r_i$  and outer radius  $r_o$  of the translator as shown in Fig. 5, and also the air gap length  $\ell_g$  and magnet thickness  $h_m$ . In order to minimise flux leakage between adjacent poles, it is desirable to have  $h_m > \ell_g$  and  $\ell_{ipg} > \ell_g$ , where  $\ell_{ipg}$  is the inter-polar gap (see Fig. 6).

### 3.2 Magnet shape

In order to have a uniform stator thickness, the magnets will be slightly tapered as shown in Fig. 5. This means that  $h_m$  will be larger on the outside ( $h_{m_o}$ ) of the machine than on the in-

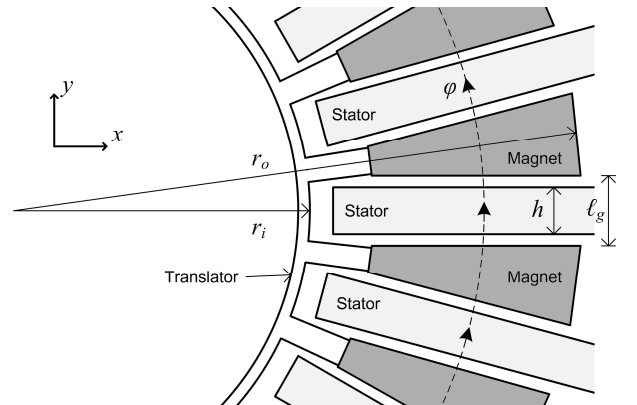


Figure 5: Top view of proposed machine.

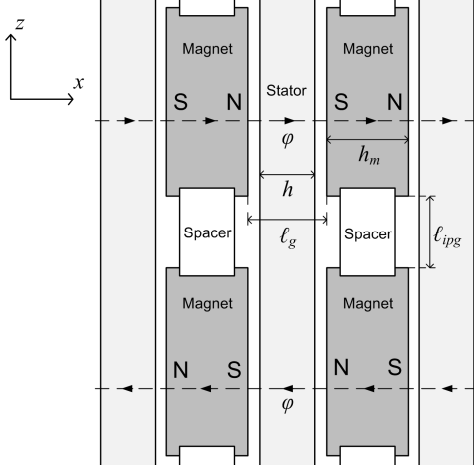


Figure 6: Side view of proposed machine.

side ( $h_{mi}$ ). Considering that the flux flows as described in Section 2 and ignoring leakage flux,

$$n_s (H_m h_m + H_g \ell_g) = 0, \quad (3)$$

where  $H_m$  and  $H_g$  are the magnetic flux intensity in the magnet and in the air gap respectively. From Equation (3) and the characteristics of the magnets, and taking  $B_p \approx B_m$ , where  $B_m$  is the magnet flux density, it can be deduced that

$$B_p = \frac{\mu_0 h_m B_r H_c}{\mu_0 h_m H_c + h_g B_r}. \quad (4)$$

It can be seen that  $B_p$  is dependent on the magnet height  $h_m$ , and will thus vary from the inside to the outside of the translator. The thickness in the middle of the magnet is used to calculate an average flux density for use in the design.

### 3.3 Winding layout

Winding factors for air-cored concentrated coil windings are thoroughly evaluated for linear machines in [6] and axial flux rotating machines in [7]. In [6], the peak induced line-to-neutral phase voltage is calculated as

$$E_p = \frac{2\omega q B_p \ell L N k_p k_d}{\pi p a}, \quad (5)$$

where  $q$  is the number of coils per phase,  $k_p$  is the pitch factor,  $k_d$  is the distribution factor,  $a$  is the number of parallel circuits,  $p$  is the number of active poles,  $N$  is the number of turns per coil,  $L$  is the active length of the machine and  $\ell$  is the active stator winding length (see Fig. 7). The highest thrust per given copper losses is achieved for a pole/coil combination of 4/3 [7], with one coil per phase per winding section ( $k_d = 1$ ) and a coil-side to coil-span ratio  $\theta_r/\theta_m = \kappa \approx 0.4$  [6].

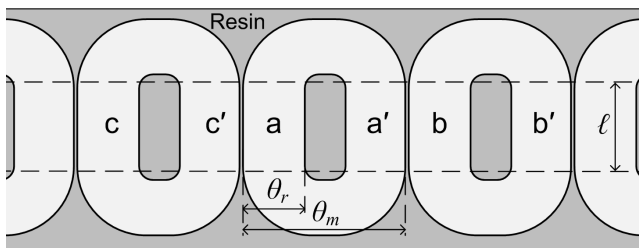


Figure 7: Non-overlapping concentrated coil winding layout.

### 3.4 Losses

Copper losses by far dominate the losses in the machine and are given by

$$P_{cu} = \frac{3}{2} I_p^2 R_{ph}, \quad (6)$$

where  $I_p$  is the peak phase current, and the phase resistance  $R_{ph}$  can be calculated as

$$R_{ph} = \frac{N^2 q \rho_{cu} (2\ell + \ell_e)}{a^2 k_f h w}, \quad (7)$$

where  $\rho_{cu}$  is the resistivity of copper,  $k_f$  is the copper fill factor and  $\ell_e$  is the average end-turn length of a coil.

It is explained in Section 3.1 that a large air gap area is needed for slow speed machines such as this. The larger air gap area unfortunately means more copper is used for a particular amount of force, and this means higher copper losses. Although increasing the current density would increase the shear stress, it will also have a quadratic increase in copper losses as an effect. It is thus important in the design to consider the trade-off between shear stress and efficiency for this machine.

The armature reaction is very small for air-cored machines and hence the eddy current losses in the magnets are neglected. However, as the flux through the stator is not concentrated in steel teeth, eddy losses are also induced in the copper wire and can be calculated, as shown in [13], by

$$P_e = 1.7 N Q n_c \frac{2\pi \ell d^4 B_p^2 \omega^2}{32 \rho_{cu}}, \quad (8)$$

where  $n_c$  is the number of parallel strands per coil turn,  $Q$  is the total number of coils and  $d$  is the wire diameter. It is important to note that  $P_e$  can be limited by making use of stranded coil turns in order to make the wire of an appropriately small diameter.

### 3.5 Machine length

Either one of the stator or the translator needs to be longer than the other in order to maintain a constant air gap during movement of the translator. Most existing machines have a PM translator which is longer than the stator in order to minimise the amount of inactive copper windings at the cost of more magnet material [12]. The question of how much the translator should be longer than the stator depends on the stroke length; this is determined by the typical wave height for which the machine is designed. In order to maintain a constant air gap area for a peak-to-peak wave amplitude of 2 m, the translator would have to be 2 m longer the stator. It may be uneconomical to construct such a stator, especially for smaller machines. It could be acceptable to allow for a smaller active air gap area near the end of the stroke, because the velocity, and hence power, is in any case at its lowest point then.

## 4 Case studies

In order to assess the viability of the concept it was decided to design two machines (referred to as N1 and N2), to compare with two existing longitudinal flux iron-cored PM machines; these are a 1 kW and a 10 kW machine from OSU [11, 12] and Uppsala University [1, 2] respectively.

### 4.1 Machine dimensions

Pole and magnet widths as well as stator and translator lengths were chosen to match those of the existing machines as closely as possible, while staying within the constraints set out in Section 3.1; these dimensions are shown in Table 1. Based on this,  $\ell_g$  was chosen as 14 mm. A 2 mm air gap was allowed on both sides of the stator, leaving the stator thickness  $h = 10$  mm. An outside radius of 0.3 m was chosen. All these dimensions were kept constant while varying the inside radius  $r_i$  in order to find the greatest air gap area. As the number of stator sections is increased, the magnet thickness decreases. The maximum number of stator sections was used while again keeping the average magnet thickness ( $h_m$ ) within the constraints of Section 3.1. Fig. 8 shows how the air gap area varies as the ratio  $\delta_d = r_i/r_o$  is varied. It is clear that the air gap area is increased for a smaller value of  $\delta_d$ , even though fewer stators are used. However, for practical reasons,  $\delta_d$  can-

Parameter	OSU	N1	Uppsala	N2
Stator core	Iron	Air	Iron	Air
Stator length $\ell_s$ (m)	0.288	0.288	1.3	1.3
Translator length $\ell_t$ (m)	1.152	1.152	1.8	1.8
Air gap area $A_g$ (m <sup>2</sup> )	0.54*	1.56	2.08	7
Poles $p$	4	4	26	26
Pole width $\theta_p$ (mm)	72	72	50	50
Magnet- to pole width ratio $\tau_m$	0.72	0.72	0.8	0.7
Frequency $f$ (Hz)	5.3	5.3	7	7
Air gap peak flux density $B_p$ (T)	0.94	0.7	1	0.7
Current density $J$ (A <sub>rms</sub> /mm <sup>2</sup> )	2.25	2.25	1.8	1.8
Electric loading $K$ (kA <sub>rms</sub> /m)	3.67*	6.8	9.72*	5.5
Shear stress $\sigma_s$ (kN/m <sup>2</sup> )	2.44*	3.4	6.87*	2.7
Shear force $f_s$ (kN)	1.315	5.3	14.29	19.1
Average velocity $v_s$ (m/s)	0.76	0.76	0.7	0.7
Power $P$ (kW)	1	4	10	13.4
Copper losses $P_{cu}$ (p.u.)	0.12*	0.2	0.1	0.16
Eddy losses $P_e$ (p.u.)	-	0.002	0.06	0.003
Efficiency $\eta$ (%)	-	79	86	84
Peak phase voltage $E_p$ (V)	346	162	163	162
Phase resistance $R_{ph}$ ( $\Omega$ )	4.58	2.05	0.4*	0.47
Copper mass $M_{cu}$ (kg)	28.55	80	70*	315
Total stator mass $M_s$ (kg)	139.4	106	836*	419
Magnet mass $M_m$ (kg)	222	504	115	754
Total translator mass $M_t$ (kg)	1446	607	547	903
Number of parallel circuits $a$	-	3	-	18

Table 1: Comparison of existing machines with two different designs of the novel topology (N1 and N2).

\* Parameters calculated from given data.

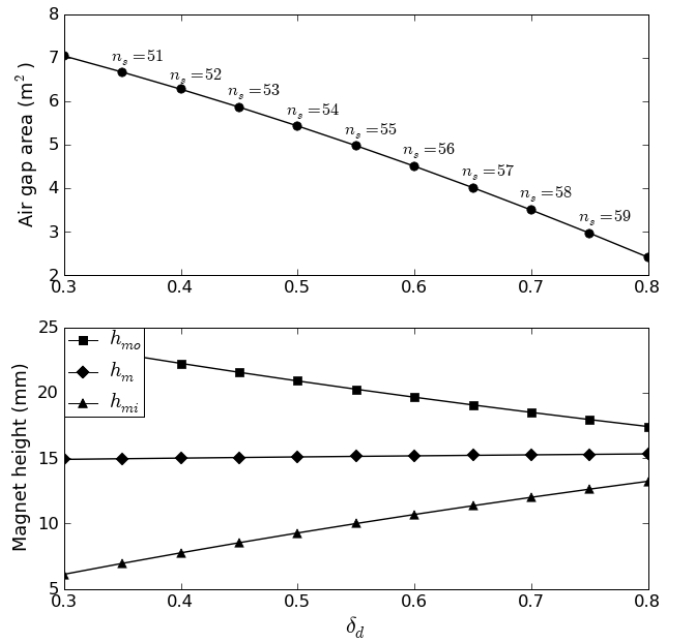


Figure 8: Air gap area optimization ( $h_g = 14$  mm,  $L = 1$  m,  $r_o = 0.3$ ).

not be too small, and a realistic ratio of 0.5 was chosen. Table 2 gives the dimensions which are common between the two case study machines.

### 4.2 Flux density

Due to the large air gap, the flux density is expected to decrease rapidly from the pole face towards the middle of the stator. A FEM package (Infolytica Magnet 7) was therefore used to verify the analytically obtained flux density. Fig. 9 shows the obtained flux density as it varies in the air gap, from one pole face to the next, at an average magnet thickness of 15 mm. The flux density as obtained here is used in further calculations.

Inner radius $r_i$ (m)	0.15	Turns per coil $N$	100
Outer radius $r_o$ (m)	0.3	Strands per turn $n_c$	10
Stator thickness $h$ (mm)	10	Number of stators $n_s$	54
Air gap length $\ell_g$ (mm)	14	Copper fill factor $k_f$	0.45

Table 2: Machine parameters which are common between N1 and N2.

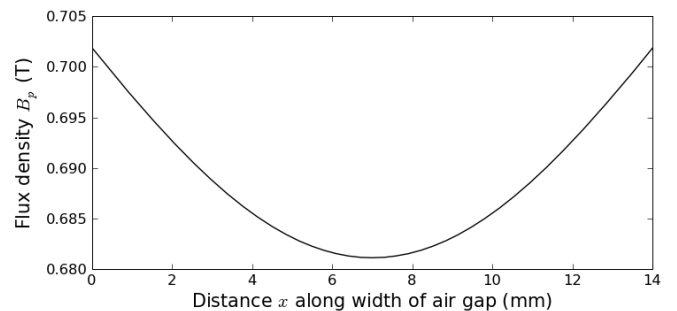


Figure 9: Flux density variation in the air gap between opposing magnet pole-faces (from FEA).

### 4.3 Winding design

The number of turns per coil determines the induced voltage and a convenient value was selected. The number of parallel strands per turn was increased in order to decrease the diameter of each strand; this is to limit the eddy losses, as was explained. All the coils of each phase in a stator section are connected in series and then different stator sections can be connected in series or in parallel; this again only serves to control the output voltage. Table 1 gives the number of parallel circuits  $a$  for each design.

### 4.4 Current density and efficiency

The current density is a parameter which needs to be selected. Usually one would select a suitable value according to the machine's thermal limitations. As explained before, though, the increased amount of copper in this machine now causes copper losses to be the limiting factor on the current density. Fig. 10 shows how N1's efficiency (neglecting  $P_e$ ) varies with current density. For a better comparison and as given in Table 1, the current densities of the existing machines are used in the case study machines.

### 4.5 Discussion

A number of aspects regarding the dimensional and performance parameters of the different machines in Table 1 are worth noting:

1. For the same active length of the machine, a 190 - 240 % increase in air gap area is achieved with the novel topology.
2. The Uppsala machine compensates for a smaller air gap area with a much larger shear force, which is due to a higher electrical loading. The deep slots of this machine allow for more ampere-turns per unit length. At the same current density, an output power improvement of 34 % is achieved with N2, but with a slightly lower efficiency.
3. In comparison with the OSU machine, a 300 % higher output power is achieved at the same current density, but at a very poor efficiency of 79 %. However, with a much lower current density of  $1 \text{ A}_{\text{rms}}/\text{mm}^2$ , the output power is still 80 % higher than in the OSU machine, but now has an efficiency of 90 % (see Fig. 10).

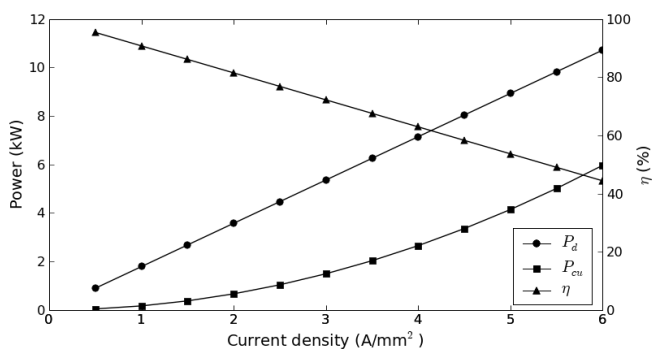


Figure 10: Efficiency as a function of current density for N1.

4. Significantly more copper is used in the air-cored machines. Although the iron-cored machines have deeper slots, the increased air gap area and amount of inactive copper in the end windings of the air-cored machines cause this topology to use much more copper. This also causes the copper losses of the air-cored machines to be higher.
5. The magnet mass of the air-cored machines is up to 560 % higher than what is used for the iron-cored machines. This will have a big cost implication. However, because the novel topology has no translator yoke and the support structure can be constructed from low density, non-magnetic materials, the total translator mass of the different machines are more comparable.
6. Even though more copper is used in the air-cored machines, the absence of steel in their stators results in a total mass that is much lower than the iron-cored stators' mass.

Although these air-cored design parameters are not optimised, the case studies show that the novel topology with an air-cored stator is comparable to existing iron-cored machines. Further studies will focus on design optimisation to minimise copper and magnet material usage and limit copper losses.

## 5 Longitudinal end effect

The longitudinal end effect as described in Sections 1 and 2 should be eliminated using this topology by eliminating the pair wise flux coupling between adjacent magnet poles. In order to verify this, more FEM studies were done. The flux distribution along the length of a 4 pole translator was investigated. Fig. 11 shows the flux lines along the top two poles of the machine and Fig. 12 shows the flux density along the vertical length ( $z$ -direction) of the air gap for the entire translator. It is clear that the flux in the top pole is the same as in the adjacent pole (Fig. 11) and that the flux is evenly distributed along the entire length of the machine (Fig. 12). This topology therefore successfully eliminates pair-wise flux coupling between adjacent poles.

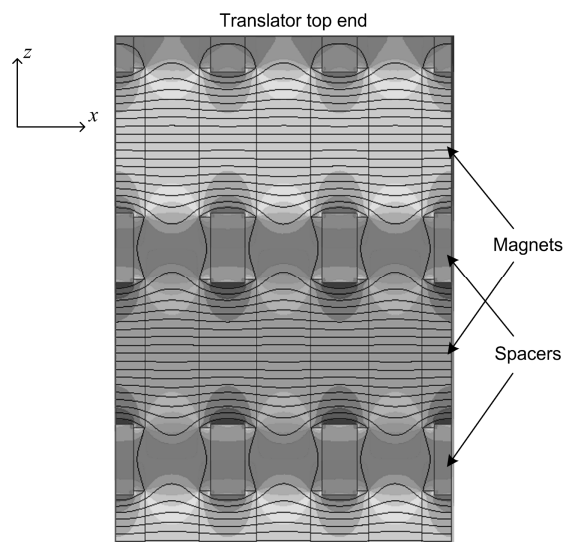


Figure 11: Flux set-up in new proposed linear PM machine.

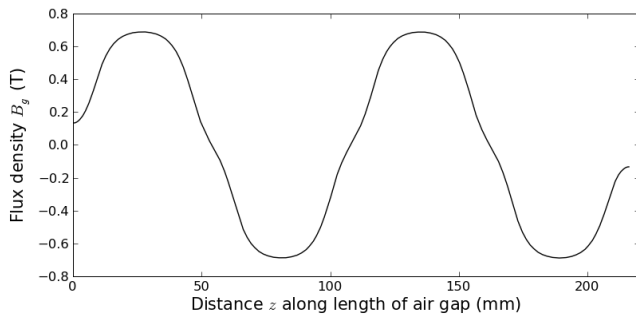


Figure 12: Flux density along the vertical length of the air gap.

## 6 Conclusion

A novel topology of a permanent magnet linear generator for ocean wave energy conversion is introduced in concept. In this topology, the stator and translator yokes are removed and a new flux path introduced. The concept is analysed analytically and with FEM simulation.

Two air-cored designs are compared with existing similarly dimensioned iron-cored machines. It is found that a larger air gap area and power density can be achieved with the novel topology, but much more magnet material and copper are used and that efficiency can be adversely affected by high copper losses. However, decreasing current density can reduce copper losses while power output is still better than in existing machines; and due to the elimination of a steel translator yoke, the total translator mass is still comparable to existing machines. FEA confirms that the longitudinal end effect associated with linear machines is eliminated with this topology.

The yoke-less air-cored stator is also much lighter than the iron-cored stators. Furthermore, the modular stator sections with their concentrated coils can significantly simplify construction and hence reduce construction time and cost. With an air-cored stator there is also no cogging force, and hence a high quality force and induced voltage waveform is achieved.

For a detailed comparison of different machines, structural mass should also be taken into account; this is ignored in this study though. However, due to the topology of this machine, the net attraction force on magnets are ideally zero and, also, because of the air-cored stator, attraction forces between the stator and translator are eliminated. It is therefore reasonable to expect structural mass for this topology to be significantly less than in conventional machines.

## Acknowledgements

The financial assistance of the South African National Energy Research Institute towards this research is hereby acknowledged. Opinions expressed and conclusions arrived at, are those of the author and are not necessarily to be attributed to SANERI.

## References

- [1] O. Danielsson, *Wave Energy Conversion. Linear Synchronous Permanent Magnet Generator*. PhD Thesis, Uppsala, Sweden: Uppsala University, (2006).
- [2] O. Danielsson, M. Eriksson, and M. Leijon, "Study of a longitudinal flux permanent magnet linear generator for wave energy converters," *Int. J. Energy Res.*, **30**, pp. 1130-1145, (2006).
- [3] O. Danielsson and M. Leijon, "Flux distribution in linear permanent magnet synchronous machines including longitudinal end effects," *IEEE Trans. on Magnetics*, **43**, (7), pp. 3197-3201, (2007).
- [4] J. Falnes, "A review of wave-energy extraction," *Marine Structures*, **20**, pp. 185-201, (2007).
- [5] N. Hodgins, A. McDonald, J. Shek, O. Keysan, and M. Mueller, "Current and Future Developments of the C-GEN Lightweight Direct Drive Generator for Wave & Tidal Energy," in *Proc. 8th Euro. Wave & Tidal Energy Conference*, Uppsala, Sweden, (2009), pp. 352-359.
- [6] M. J. Kamper, "Comparison of linear permanent magnet machine with overlapping and non-overlapping air-cored stator windings," in *Proc. IET 4th Int. Conf. Power Electronics, Machines and Drives*, York, UK, (2008), pp. 767-771.
- [7] M.J. Kamper, R.-J. Wang, and F.G. Rossouw, "Analysis and performance of axial flux permanent-magnet machine with air-cored nonoverlapping concentrated stator windings," *IEEE Trans. Industry Applications*, **44**, (5), pp. 1495-1504, (2008).
- [8] M. A. Mueller, H. Polinder, and N. Baker, "Current and novel electrical generator technology for wave energy converters," in *Proc. IEEE Int. Electrical Machines and Drives Conf.*, **2**, Antalya, Turkey, (2007), pp. 1401-1406.
- [9] H. Polinder, M. J. Hoeijmakers, and M. Scuotto, "Eddy-current losses in the solid back-iron of PM machines for different concentrated fractional pitch windings," in *Proc. IEEE Int. Electrical Machines and Drives Conf.*, **1**, Antalya, Turkey, (2007), pp. 652-657.
- [10] H. Polinder, M. A. Mueller, M. Scuotto, and M. Goden de Sousa Prado, "Linear generator systems for wave energy conversion," in *Proc. 7th Euro. Wave & Tidal Energy Conference*, Porto, Portugal, (2007).
- [11] J.H. Prudell, *Novel design and implementation of a permanent magnet linear tubular permanent magnet generator for ocean wave energy conversion*, MS Thesis, Corvallis, USA: Oregon State University, (2007).
- [12] J. Prudell, M. Stoddard, T.K.A. Brekken, and A. von Jouanne, "A novel permanent magnet tubular linear generator for ocean wave energy," in *Proc. IEEE Energy Conversion Congress & Exposition*, San Jose, CA, (2009), pp. 3641-3646.
- [13] R.-J. Wang and M.J. Kamper, "Calculation of eddy current loss in axial field permanent-magnet machine with coreless stator," *IEEE Trans. Energy Convers.*, **19**, (3), pp. 532-538, (2004).